

Analysis of the Origin of Cardiac Wall Motion that Constitutes Myocardial
Velocity-Time Curves in Patients with Left Bundle Branch Block

Yoshihiro Seo, MD, Tomoko Ishizu, MD, Fumiko Sakamaki, RDMS, Masahiro Yamamoto, MD,
Tomoko Machino, MD, Shigeyuki Watanabe, MD, Kazutaka Aonuma, MD
Cardiovascular Division, Graduate School of Comprehensive Human Science, University of
Tsukuba, Ibaraki, Japan

Corresponding author:

Yoshihiro Seo, MD

Cardiovascular Division

Graduate School of Comprehensive Human Science

University of Tsukuba

1-1-1 Tennodai

Tsukuba 305-8575, JAPAN

Phone: +81-298-53-3142

Fax: +81-298-53-3143

E-mail: yo-seo@md.tsukuba.ac.jp

Abstract

Septal and lateral wall myocardial velocity-time curves from tissue Doppler imaging were analyzed to determine wall motion from which the velocity originated in 34 patients with left bundle branch and systolic dysfunction (ejection fraction <45%). Longitudinal strain rate by speckle tracking imaging was assessed to identify whether corresponding wall motion was active or passive. All lateral peak velocities during the ejection period were derived from delayed active movement. However, septal peak velocities (V_{sp}) were more numerous and complex. V_{sp} during pre-ejection was derived from first active movement in 29 patients (85.2%). V_{sp} during the ejection period was derived from second active movement in 20 patients, passive movement in 9 patients, and first active movement in only 5 patients. Because V_{sp} was consistent with various wall motion types, identification of V_{sp} origin including that during pre-ejection may be important in identifying LV dyssynchrony based on propagation of first active myocardial movements.

Cardiac resynchronization therapy (CRT) is an established non-pharmacologic therapy for patients with advanced heart failure and cardiac dyssynchrony.¹⁻³ Detection of cardiac dyssynchrony by Doppler echocardiography has focused on identifying responders to CRT.⁴⁻⁹ In particular, tissue Doppler imaging (TDI) has been central to the detection of cardiac dyssynchrony,⁵⁻⁸ however, recent studies have shown results that negate the utility of TDI in identifying left ventricular (LV) dyssynchrony and CRT responders.^{10,11} Assessments of cardiac dyssynchrony with TDI have been performed by analysis of myocardial velocity-time curves, in which the analysis period has been limited to the ejection period.⁵⁻⁸ However, myocardial velocity-time curves have multiple peaks and vary throughout the systolic phase in individual patients. Although the theoretical effect of CRT is to modify the mechanical dyssynchrony of active myocardial motion, not passive motion, with electrical resynchronization, TDI-derived velocities alone cannot distinguish active from passive wall motion.¹² Thus, the wall motion from which the velocities originate has not been identified. We hypothesized that identification of the origin of tissue velocity peaks would be useful to detect cardiac dyssynchrony of active wall motion and that this knowledge can contribute to more accurate prediction of CRT responders than can be derived from TDI velocity information alone. Therefore, the aim of this study was to identify the origin of cardiac wall motion that constitutes myocardial velocity-time curves in patients with LV dysfunction and complete left bundle branch block (CLBBB).

METHODS

Patients

Thirty-four patients (18 men and 16 women; mean age, 61 ± 15 years) with CLBBB (QRS duration >120 ms) and LV dysfunction (LV ejection fraction $<45\%$) were enrolled in this study. Baseline characteristics of the patients are presented in Table 1. Patients were in New York Heart Association (NYHA) class II ($n = 6$), III ($n = 22$), or IV ($n = 4$) heart failure. The intrinsic rhythm in all patients was sinus rhythm. The project was approved by the local research ethics committee, and the patients gave their written informed consent.

Echocardiography

All Doppler echocardiographic examinations were performed with a Vivid 7 system (GE Vingmed Ultrasound, Horten, Norway) equipped with a multifrequency transducer. LV end-diastolic volume (LVEDV), LV end-systolic volume (LVESV), and LV ejection fraction (EF) were measured using a modified Simpson's method.¹³

Color-coded TDI

Color-coded TDI images were obtained in apical 4-chamber views. The image sector was set as narrow as possible, which resulted in a frame rate greater than 100 frames/s, and a cine-loop of 3 consecutive beats was stored for later off-line analysis on a workstation using a software package (EchoPac 6.3.6, GE Medical Systems, Horten, Norway). Myocardial pulsed Doppler velocity profile signals were reconstituted offline from the color-coded TDI images that provided regional myocardial velocity-time curves derived from the sample area positioned at the basal LV myocardium.¹⁴ In patients with a markedly dilated LV, the most basal part of the LV wall bends inward, and consequently the ultrasound beam is at a large angle with the wall.¹⁵ Therefore, the

sample volume was placed at the apical site of the basal segment to be as parallel as possible to the central ultrasound beam. Myocardial velocity-time curve assessment was done for the pre-ejection period, ejection period, and isovolumic relaxation time (IRT).

Speckle Tracking Imaging

We scanned the same apical 4-chamber views using speckle tracking imaging (STI) to assess regional strain rate values, which were used to identify the TDI-derived peak myocardial velocities from active or passive wall motion because strain rates based on STI may be more accurate than those based on TDI measurements.¹⁶ STI was performed as soon as possible after TDI scanning. The frame rate was adjusted to greater than 35 frames/s, and cine loops of 3 consecutive beats were stored for off-line analysis on the workstation.⁹ Longitudinal STI was assessed on the workstation as follows: first, the endocardium was traced on an end-systolic frame, and a region of interest was automatically selected to approximate the myocardium between the endocardium and epicardium. The width of the region of interest was adjusted to the wall thickness. The software then captured the myocardium, automatically tracked its motion and thickening on the subsequent frames, and divided the longitudinal image into 6 segments.¹⁷ Longitudinal strain rate values from multiple longitudinal points were calculated, and the data was averaged into 6 segmental myocardial strain rate-time curves.

Definition of Active and Passive Wall Motion

We carefully compared the myocardial velocity-time curve from TDI with the longitudinal strain rate-time curve from STI because the cardiac cycle used to assess TDI was different from that used to assess STI. We defined the peak positive velocity component in which the corresponding longitudinal strain rate value was negative as

active wall motion and the component with positive strain rate as passive wall motion (Figures 1, 2).¹²

Propagation of Myocardial Contraction

We measured the time differences from septal peak velocities to lateral peak velocities to assess the propagation of myocardial contraction. We assessed two types of time differences. First, the period investigated was limited to the ejection period regardless of active or passive wall motion. Second, the time differences were measured between the first septal and the first lateral peak derived from the first active wall motion in all investigation periods.

Reproducibility

We investigated intra- and inter-observer agreement of the diagnosis of active or passive movements with Cohen's κ coefficients. Inter-observer agreement was independently assessed by 2 observers (Y.S. and F.S.).

Statistical Analysis

Results are expressed as the mean value \pm SD. Comparisons between groups were performed with Student's *t*-test for continuous variables and the χ^2 test for categorical variables. A *P* value <0.05 was considered to indicate statistical significance. All calculations were performed with the Dr. SPSS II for Windows statistical program (SPSS Inc., Chicago, IL).

RESULTS

Appropriate images for analysis could be obtained in all patients. Two representative cases are shown. In the first case (Figure 1), all septal peaks had negative longitudinal strain rate values at the corresponding points in the longitudinal strain rate-time curve,

indicating that all septal peaks were derived from active septal wall motion. Note that the peak during the ejection phase was derived from the second active wall motion, not the first active motion. In the second case (Figure 2), the first septal peak was observed during the pre-ejection period and had a negative longitudinal strain rate value at the corresponding point, followed by the first lateral peak, which had a positive longitudinal strain rate value at the corresponding point. Thus, the septal peak was derived from the first active wall motion in the septum, and the lateral peak was derived from passive lateral wall motion. The second peaks in both myocardial velocity-time curves were observed during the ejection phase. The second lateral peak had a negative longitudinal strain rate value at the corresponding point, followed by the second septal peak, which had a positive longitudinal strain rate value at the corresponding point. In contrast to the pre-ejection phase, the second lateral peak was derived from active lateral wall motion, and the second septal peak was derived from passive septal wall motion. Thus, interestingly, active wall motion and passive wall motion in the opposite walls were linked and occurred in sequence. Corresponding color-coded myocardial velocity images are shown in Figure 3.

The timing and sequence of velocity peaks are summarized in Figure 4. During the investigated periods, the total number of peaks was 84 in the septal wall and 62 in the lateral wall. The average number of velocity peaks in the myocardial velocity-time curves were significantly greater in the septal wall curves than in the lateral wall curves (2.5 ± 0.6 peaks vs. 1.8 ± 0.7 peaks, $P < 0.001$). In the septal wall curves, most of the first peaks derived from active septal wall motion were observed during the pre-ejection period (29 patients; 85.3%). In contrast, the first peaks derived from active septal wall motion in the 5 remaining patients were observed during the ejection period. Most of

the peak velocities during the ejection period in the septal myocardial velocity-time curves were derived from second active septal motion (20 patients) and passive septal motion (8 patients). Fourteen patients with second active motion during the ejection period, 2 patients with passive septal motion, and 2 patients with first peak during the ejection period had a third velocity peak, which was observed during the IRT in the 14 patients and during the ejection period in the other 4 patients. In the lateral wall myocardial velocity-time curves, the first peak derived from active lateral wall motion was observed during the ejection period in all patients, although all 18 velocity peaks occurring during the pre-ejection periods were determined deriving from passive wall motion. Six patients had three velocity peaks.

When investigation was limited to the ejection periods, regardless of active or passive wall motion, the time differences were varied (17.7 ± 33.4 ms, range -56.0 to 78.0 ms, Figure 5). The time differences were negative in 10 patients; the lateral peak was earlier than the septal peak. In contrast, when the time differences were measured between the first septal and the first lateral peak derived from active wall motion during the investigated periods, the time differences were positive in all patients (51.1 ± 21.3 ms, range 12.0 to 112.0 ms). Even in the 24 patients with a positive value at the first investigation, the time differences increased in the half of patients (19.7 ± 20.3 ms, range 2.0 to 67.0 ms vs. 50.5 ± 30.0 ms, range 34.0 to 112.0 ms).

Reproducibility

Cohen's κ coefficient of intra-observer agreement of diagnosis of active or passive movements was 0.83, and that of inter-observer agreement was 0.81.

DISCUSSION

The present study showed that myocardial velocity-time curves consist of various types of wall motion, especially within the septal wall in patients with CLBBB. The first peak velocity derived from initiation of active septal wall motion was observed during the pre-ejection period in most patients, whereas the first lateral peak velocity was observed during the ejection period. Therefore, in patients with LBBB, the septal peak velocity during the pre-ejection period should be included to assess the dyssynchrony of active contraction because TDI-derived myocardial velocity may not distinguish active contraction from passive wall motion.

The present study showed that the septal myocardial velocity-time curve had multiple peaks that were derived from various types of wall motion. Multiple types of wall motion in the septum have been reported in early M-mode echocardiography studies and recent cardiac magnetic resonance imaging studies.¹⁸⁻²⁰ In patients with LBBB, the septal wall, which is the region activated earliest in the pre-ejection period, starts to shorten early, and wall motion here is often observed as a weak contraction. Weak pre-ejection motion has been reported as a passive motion caused by interventricular pressure difference.¹⁸ However, recent tagged magnetic resonance imaging studies showed this early active motion to be active contraction.²⁰ The present study showed the second septal peaks during the ejection period to be derived from a second active septal motion or passive wall motion. The origin and mechanism of this second active movement has not been identified; however, it might be related to interaction of the left and right ventricles in combination with the weak contraction following early activation of the septum. In addition, the septal and LV electronic activation sequences in patients with LBBB are variable, which may be related to multiple septal contraction patterns.²¹

We also found that passive septal wall motion is the other origin of the septal second peak. As shown in the second case, active and passive wall motion at the opposite wall were linked and in sequence during the pre-ejection and ejection periods. Paired active and passive wall motion has been known to cause a discoordinated and inefficient contraction pattern in patients with LBBB.²² Namely, early septal wall motion stretches the opposite lateral wall with which it is in sequence, thus creating passive wall motion of the lateral wall. Consequently, the prestretched lateral wall starts to shorten when all regions are activated, whereas the opposite septal wall has already finished contracting. The septal wall is now stretched because it is opposite the lateral wall, resulting in passive wall motion of the septal wall. In addition, the passive outward motion, the so-called shuffle motion between the septal and lateral walls, that is observed in the apical 4-chamber views causes longitudinal velocity toward the apex.²³ This paired conflict in wall motion between the septal and lateral walls is the underlying mechanism of LV dysfunction in patients with LBBB. However, passive wall motion cannot be distinguished from active wall motion on TDI velocity curves. Indeed, as shown in case 2, the lateral peak velocity during the ejection period often preceded the septal peak velocity, which may be the second active motion or passive wall motion. A previous study showed that TVI indicated a delayed contraction of the lateral wall in only 66% of the patients with LBBB.²⁴ These results are consistent with those of our study (70.6%). These observations suggest that the timing of peak velocity alone cannot determine the latest activated region to be the true latest region in the propagation of the activation wavefront.

In the present study, when peak velocities derived from the first active wall motion were assessed, TDI appeared to indicate mechanical propagation from the septal to

lateral wall. In patients with LBBB, the electrical activation sequence shows septal breakthrough first, with latest activation in the basal lateral or posterior wall, independently of ischemic or non-ischemic etiology.²¹ Similarly, a previous study with tagged magnetic resonance imaging showed that the contraction sequence propagated consistently from the septum to the lateral wall in non-ischemic patients.²⁰ In contrast, although other contraction sequences were observed in some of the ischemic patients, the primary contraction sequence was from the septal to lateral wall.²⁰ This is the most important propagation sequence in patients with LBBB, given that the primary effect of CRT is the mechanical resynchronization of the onset of active myocardial contraction by electrical resynchronization. Thus, the target of dyssynchrony assessments should be the first active wall motion, not the second active or passive wall motion.

Clinical Implications

Our concept that dyssynchrony should be assessed by focusing on regional first active wall motion shows that the septal myocardial velocity curve should be carefully analyzed because the lateral peak velocity during the ejection period could be the surrogate of lateral delayed wall motion; the pre-ejection period should be included when assessing the septal wall activation, and strain rate imaging should be used to differentiate first active septal wall motion from second wall motion including passive wall motion.

Limitations

First, this study consisted of a relatively small number of subjects, and further study will be needed to confirm the dyssynchrony pattern observed with our method in various patients with and without intraventricular conduction delay. Second, because we used STI to assess strain rate analysis, the cardiac cycle used in assessing TDI was different

from that used in assessing STI. Despite careful comparison between the myocardial velocity-time curve of TDI and the longitudinal strain rate-time curve of STI, the difference in cardiac cycles might have affected our results. Finally, because the region of interest of STI consisted of 3 continuous segments (base, mid, and apex) in each wall, STI-derived strain rate might not come from the exact same region of interest as that of TVI. This methodological difference may affect the STI-derived strain rate value. Further study will be needed to confirm the ability of our dyssynchrony measurement method based on propagation of the first active wall motion to select CRT responders.

Conclusions

In contrast to lateral myocardial velocity-time curves, septal myocardial velocity-time curves were varied. The septal peak velocities derived from first active septal wall motion were observed during the pre-ejection period in most patients, although septal peaks during the ejection period were derived from various types of septal wall motion including passive wall motion. When dyssynchrony is assessed in patients with LBBB on the basis of electromechanical dyssynchrony, the sequence may be represented more exactly with TDI by assessing the propagation of the first peak derived from active wall motion, and not only the ejection period but especially the pre-ejection period should be examined.

References

- 1 Abraham WT, Fisher WG, Smith AL, Delurgio DB, Leon AR, Loh E, et al. MIRACLE Study Group. Multicenter InSync Randomized Clinical Evaluation. Cardiac resynchronization in chronic heart failure. *N Engl J Med* 2002;346:1845-1853.
- 2 Bristow MR, Saxon LA, Boehmer J, Krueger S, Kass DA, De Marco T, et al. Comparison of Medical Therapy, Pacing, and Defibrillation in Heart Failure (COMPANION) Investigators. Cardiac-resynchronization therapy with or without an implantable defibrillator in advanced chronic heart failure. *N Engl J Med* 2004;350:2140-50.
- 3 Cleland J, Daubert JC, Erdmann E, Freemantle N, Gras D, Kappenberger L, et al. Cardiac Resynchronization-Heart Failure (CARE-HF) Study Investigators. The effect of cardiac resynchronization on morbidity and mortality in heart failure. *N Engl J Med* 2005;352:1539-49.
- 4 Pitzalis MV, Iacoviello M, Romito R, Massari F, Rizzon B, Luzzi G, et al. Cardiac resynchronization therapy tailored by echocardiographic evaluation of ventricular asynchrony. *J Am Coll Cardiol* 2002;40:1615-22.
- 5 Yu CM, Chau E, Sanderson JE, Fan K, Tang MO, Fung WH, et al. Tissue Doppler echocardiographic evidence of reverse remodeling and improved synchronicity by simultaneously delaying regional contraction after biventricular pacing therapy in heart failure. *Circulation* 2002;105:438-45.
- 6 Bader H, Garrigue S, Lafitte S, Reuter S, Jaïs P, Haïssaguerre M, et al. Intra-left ventricular electromechanical asynchrony. A new independent predictor of severe

- cardiac events in heart failure patients. *J Am Coll Cardiol* 2004;43:248-56.
- 7 Bax JJ, Bleeker GB, Marwick TH, Molhoek SG, Boersma E, Steendijk P, et al. Left ventricular dyssynchrony predicts response and prognosis after cardiac resynchronization therapy. *J Am Coll Cardiol* 2004;44:1834-40.
 - 8 Yu CM, Fung JW, Zhang Q, Chan CK, Chan YS, Lin H, et al. Tissue Doppler imaging is superior to strain rate imaging and postsystolic shortening on the prediction of reverse remodeling in both ischemic and nonischemic heart failure after cardiac resynchronization therapy. *Circulation* 2004;110:66-73.
 - 9 Suffoletto MS, Dohi K, Cannesson M, Saba S, Goresan J 3rd. Novel speckle-tracking radial strain from routine black-and-white echocardiography images to quantify dyssynchrony and predict response to cardiac resynchronization therapy. *Circulation* 2006;113:960-8.
 - 10 Chung ES, Leon AR, Tavazzi L, Sun JP, Nihoyannopoulos P, Merlino J, et al. Results of the Predictors of Response to CRT (PROSPECT) trial. *Circulation* 2008;117:2608-16.
 - 11 Miyazaki C, Powell BD, Bruce CJ, Espinosa RE, Redfield MM, Miller FA, et al. Comparison of echocardiographic dyssynchrony assessment by tissue velocity and strain imaging in subjects with or without systolic dysfunction and with or without left bundle-branch block. *Circulation* 2008;117:2617-25.
 - 12 Mele D, Pasanisi G, Heimdal A, Cittanti C, Guardigli G, Levine RA, et al. Improved recognition of dysfunctional myocardial segments by longitudinal strain rate versus velocity in patients with myocardial infarction. *J Am Soc Echocardiogr* 2004;17:313-21.

- 13 Schiller NB, Shah PM, Crawford M, DeMaria A, Devereux R, Feigenbaum H, et al. Recommendation for quantification of the left ventricle by two-dimensional echocardiography. American Society of Echocardiography Committee on Standards, Subcommittee on Quantitation of Two-Dimensional Echocardiograms. *J Am Soc Echocardiogr* 1989;2:358–67.
- 14 Pai RG, Gill KS. Amplitudes, durations, and timings of apically directed left ventricular myocardial velocities: I. Their normal pattern and coupling to ventricular filling and ejection. *J Am Soc Echocardiogr* 1998;11:105-11.
- 15 De Boeck BW, Meine M, Leenders GE, Teske AJ, van Wessel H, Kirkels JH, et al. Practical and conceptual limitations of tissue Doppler imaging to predict reverse remodelling in cardiac resynchronisation therapy. *Eur J Heart Fail* 2008;10:281-90.
- 16 Ingul CB, Torp H, Aase SA, Berg S, Stoylen A, Slordahl SA. Automated analysis of strain rate and strain: feasibility and clinical implications. *J Am Soc Echocardiogr* 2005;18:411-8.
- 17 Perk G, Tunick PA, Kronzon I. Non-Doppler two-dimensional strain imaging by echocardiography--from technical considerations to clinical applications. *J Am Soc Echocardiogr* 2007;20:234-43.
- 18 Little WC, Reeves RC, Arciniegas J, Katholi RE, Rogers EW. Mechanism of abnormal interventricular septal motion during delayed left ventricular activation. *Circulation* 1982;65:1486-91.
- 19 Hayashi T, Sakai Y, Kobayashi S, Ishii Y, Inoue T, Yamaguchi H, et al. Correlation between interventricular septal motion and left ventricular systolic-diastolic function in patients with left bundle branch block. *J Cardiol* 2000;35:181-7.
- 20 Zwanenburg JJ, Götte MJ, Marcus JT, Kuijjer JP, Knaapen P, Heethaar RM, et al.

- Propagation of onset and peak time of myocardial shortening in ischemic versus nonischemic cardiomyopathy: assessment by magnetic resonance imaging myocardial tagging. *J Am Coll Cardiol* 2005;46:2215-22.
- 21 Auricchio A, Fantoni C, Regoli F, Carbucicchio C, Goette A, Geller C, et al. Characterization of left ventricular activation in patients with heart failure and left bundle-branch block. *Circulation* 2004;109:1133-9.
- 22 Prinzen FW, Hunter WC, Wyman BT, McVeigh ER. Mapping of regional myocardial strain and work during ventricular pacing: experimental study using magnetic resonance imaging tagging. *J Am Coll Cardiol* 1999;33:1735-42.
- 23 Jansen AH, van Dantzig J, Bracke F, Meijer A, Peels KH, van den Brink RB, et al. Qualitative observation of left ventricular multiphasic septal motion and septal-to-lateral apical shuffle predicts left ventricular reverse remodeling after cardiac resynchronization therapy. *Am J Cardiol* 2007;99:966-9.
- 24 Breithardt OA, Stellbrink C, Herbots L, Claus P, Sinha AM, Bijnens B, et al. Cardiac resynchronization therapy can reverse abnormal myocardial strain distribution in patients with heart failure and left bundle branch block. *J Am Coll Cardiol* 2003;42:486-94.

Table 1 Baseline Characteristics

Age, yrs	61 ± 15 (range: 20-78)
Sex (male/female)	18/16
IHD/non-IHD	10/24
QRS duration	166 ± 38 (range: 130-242)
NYHA class I/II/III/IV	2/6/22/4
LVDD, mm	63 ± 10 (range: 45-82)
LVEF, %	29 ± 10 (range: 21-43)
Medications, n (%)	
β-blockers	26 (76)
ACE inhibitor/ARB	28 (83)
Diuretics	30 (88)
Digoxin	2 (6)

IHD, ischemic heart disease; *NYHA*, New York Heart Association;

LVDD, left ventricular diameter at end-diastole; *LVEF*, left ventricular

ejection fraction; *ACE*, angiotensin-converting enzyme; *ARB*,

angiotensin II receptor blocker.

Figure legends

Figure 1. Myocardial velocity-time curves (upper panel) and longitudinal strain rate-time curves with speckle tracking imaging (lower panel) from a 65-year-old man with idiopathic dilated cardiomyopathy (case 1). In the upper panel, three septal velocity peaks (yellow arrows) and one lateral velocity peak (green arrow) are seen. In the lower panel, corresponding points on the longitudinal strain rate curves are shown by dotted arrows. *MVC*, mitral valve closing; *MVO*, mitral valve opening; *AVC*, aortic valve closing; *AVO*, aortic valve opening.

Figure 2. Myocardial velocity-time curves (upper panel) and longitudinal strain rate-time curves with speckle tracking imaging (lower panel) from a 72-year-old man with prior myocardial infarction (case 2). In the upper panel, two septal velocity peaks (yellow arrows) and two lateral velocity peaks (green arrows) are shown. In the lower panel, corresponding points on the longitudinal strain rate curves are shown by dotted arrows. *AVC*, aortic valve closing; *AVO*, aortic valve opening.

Figure 3. Corresponding color-coded myocardial velocity images at early and mid systole from case 2. In early systole (left panel), weak septal upper right inward motion (yellow arrows) and lateral outward motion (green arrows) with lateral to septal apical motion (apical arrow) were observed. In contrast, at mid systole (right panel), septal upper left outward motion (yellow arrows) and stronger lateral inward motion (green arrows) with septal to lateral apical motion (apical arrow) were observed.

Figure 4. Timing, number of cases, and sequence of velocity peaks. Circles indicate the first velocity peak. Squares indicate the second velocity peak in patients with two velocity peaks, and triangles indicate the second and third velocity peaks in patients with three velocity peaks. Unfilled symbols correspond to active wall motion, and filled

symbols correspond to passive wall motion. Numbers are number of cases. *IRT*, isovolumic relaxation time.

Figure 5. Time differences from septal peak velocities to lateral peak velocities during the ejection period regardless of active or passive wall motion (left), and time differences from the first septal to the first lateral peak derived from first active wall motion for all investigated periods (right).

Figure 1

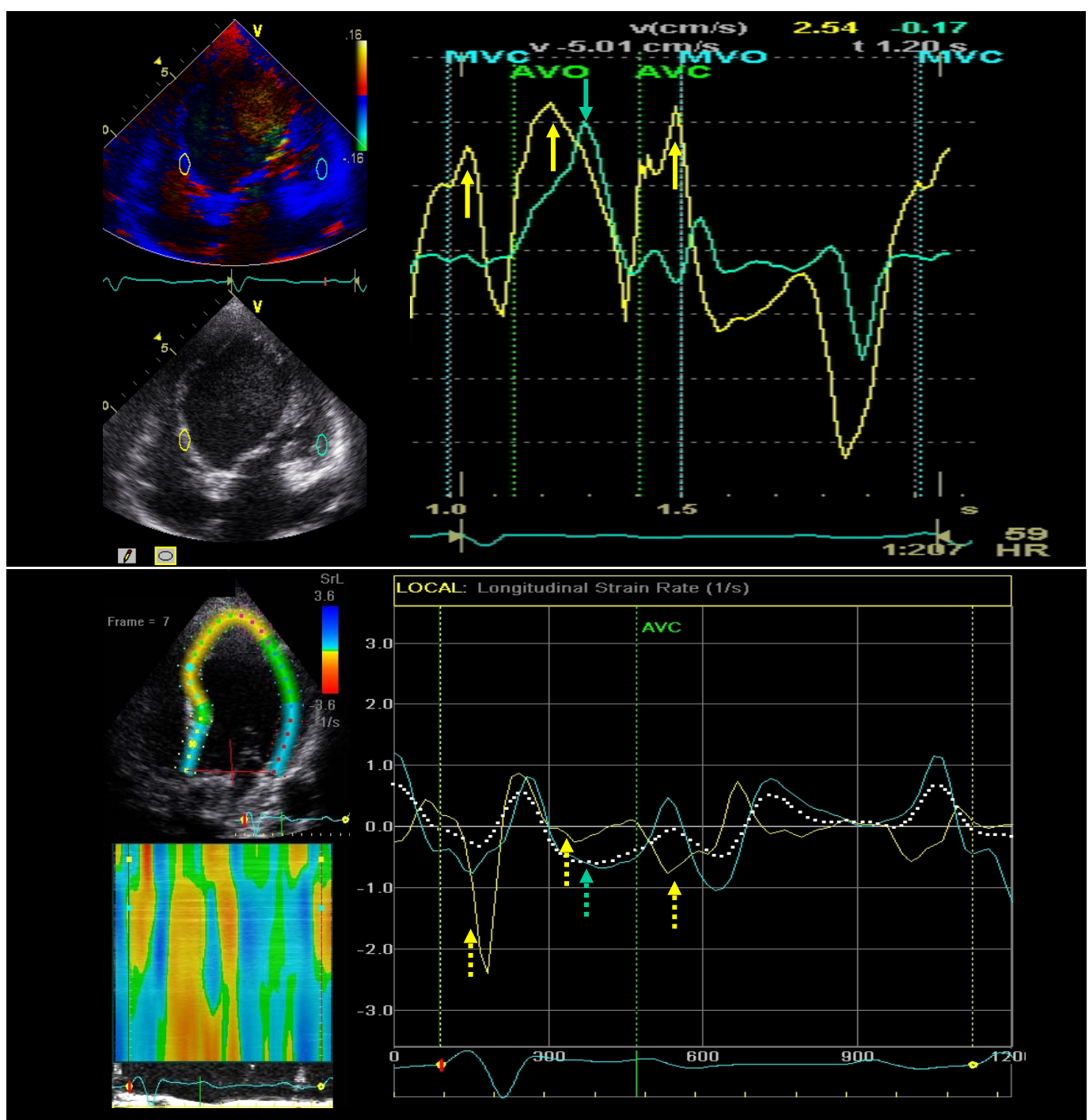


Figure 2

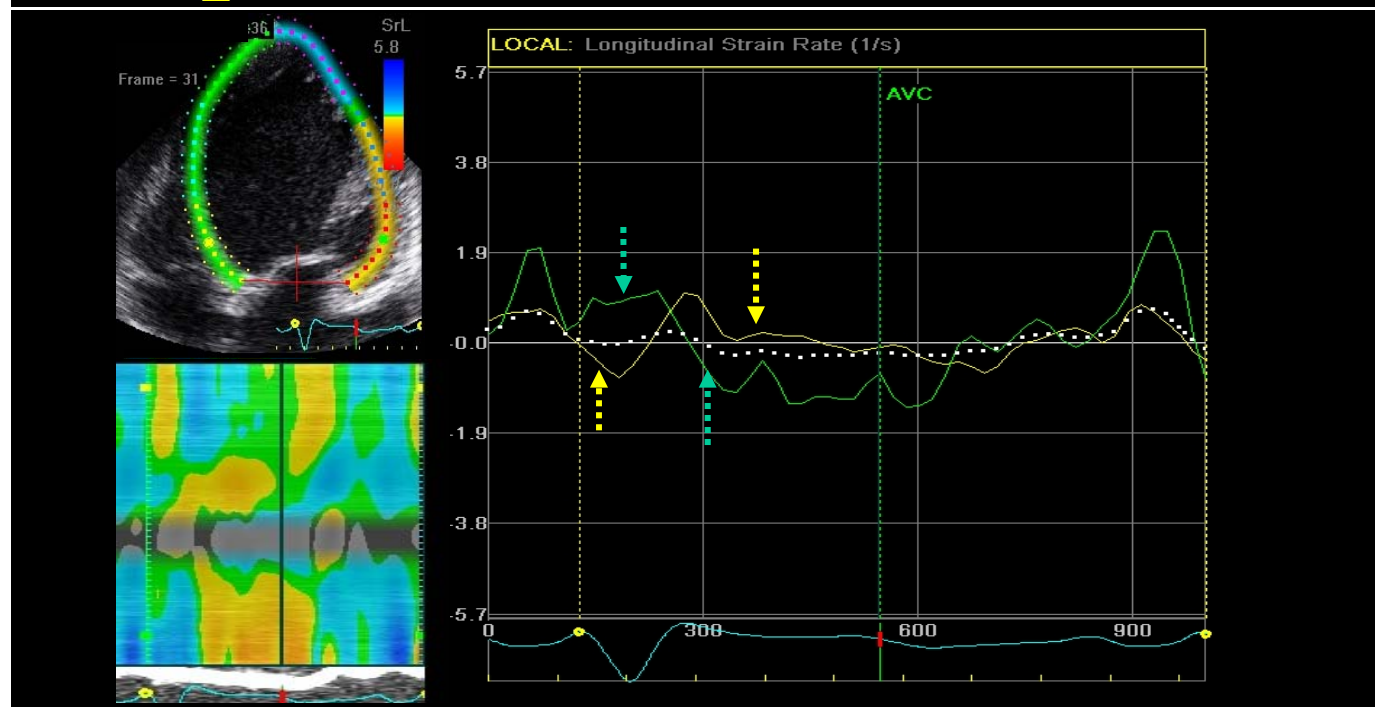
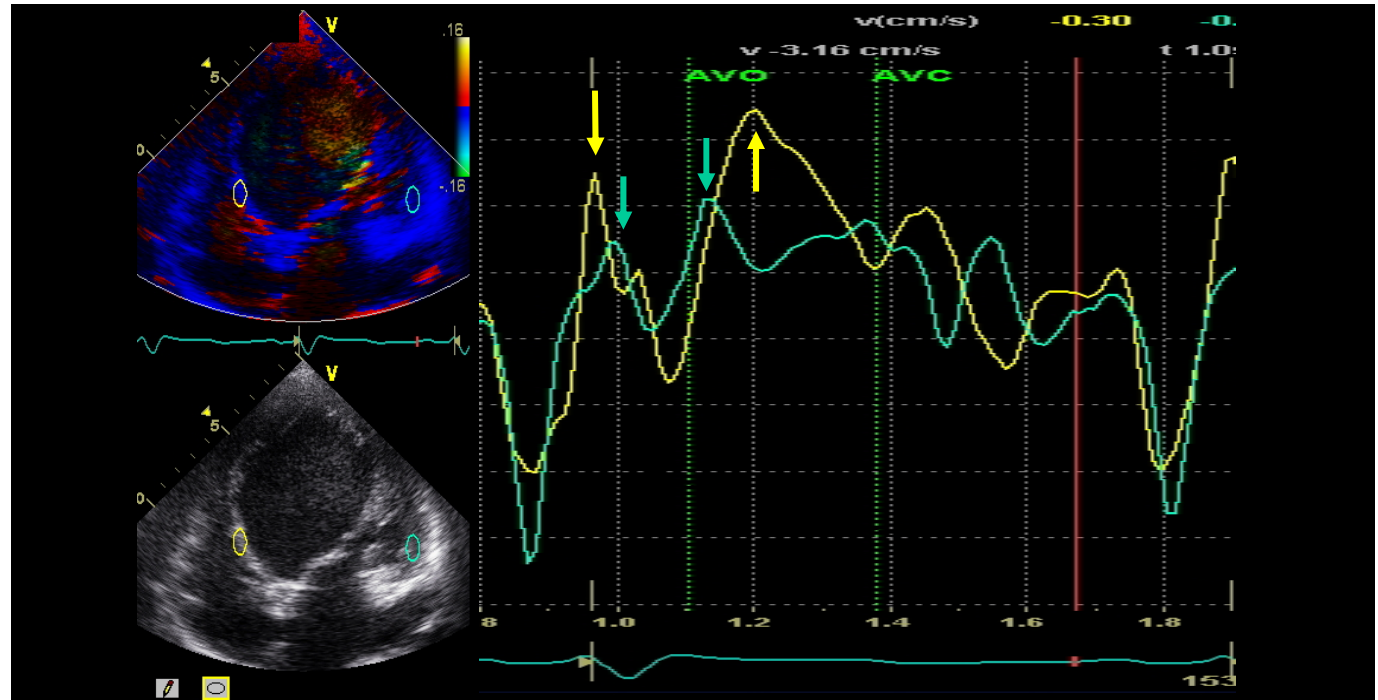


Figure 3

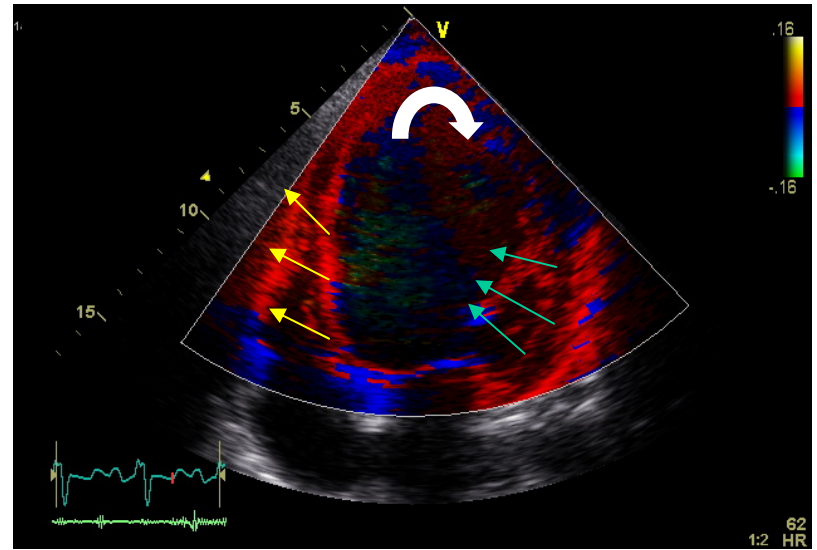
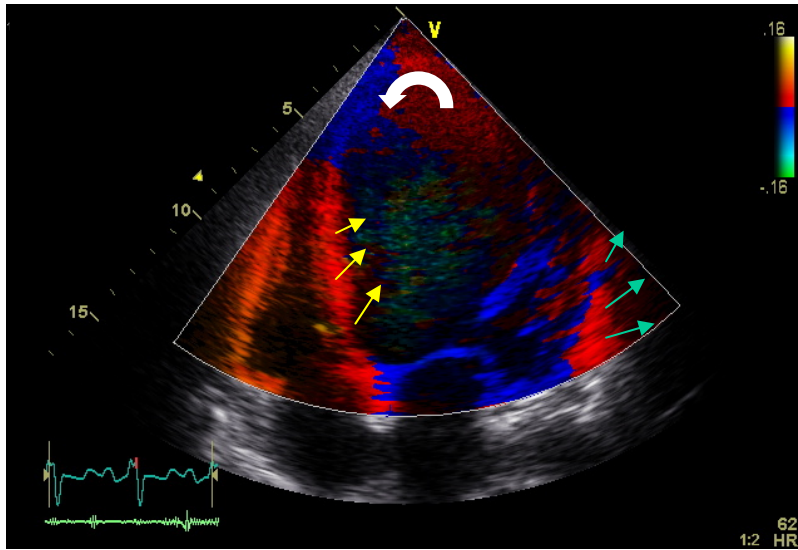


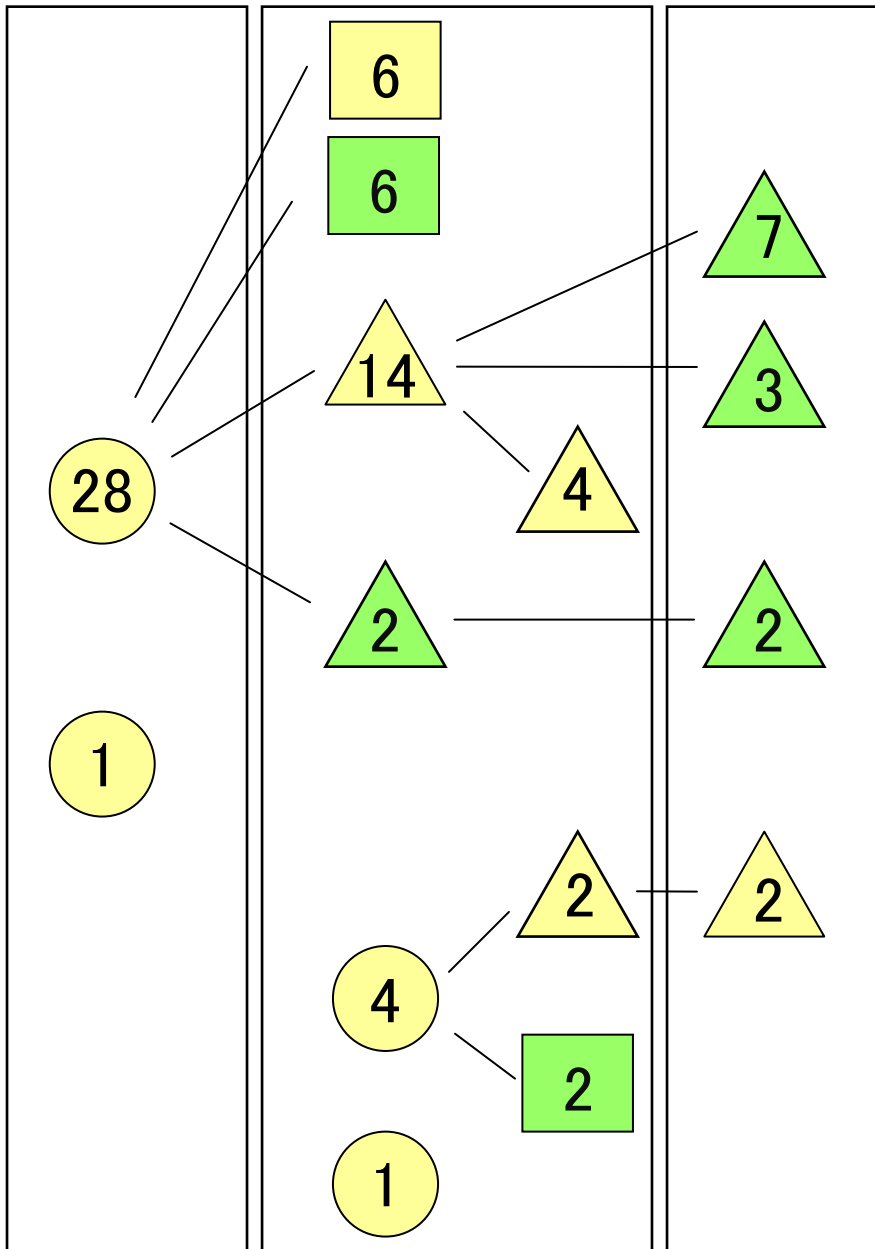
Figure 4

Septal wall

Pre-ejection

Ejection

IRT



Lateral wall

Pre-ejection

Ejection

IRT

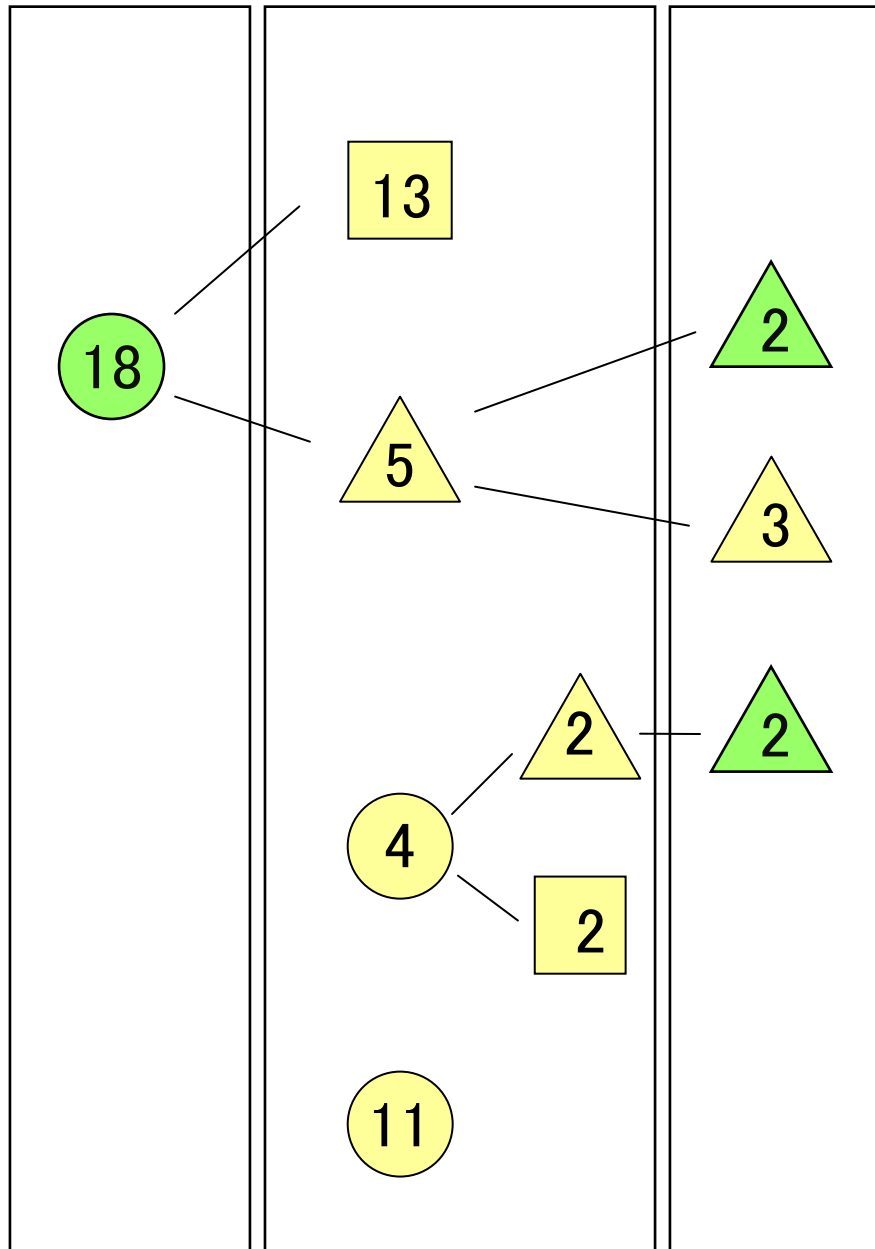


Figure 5

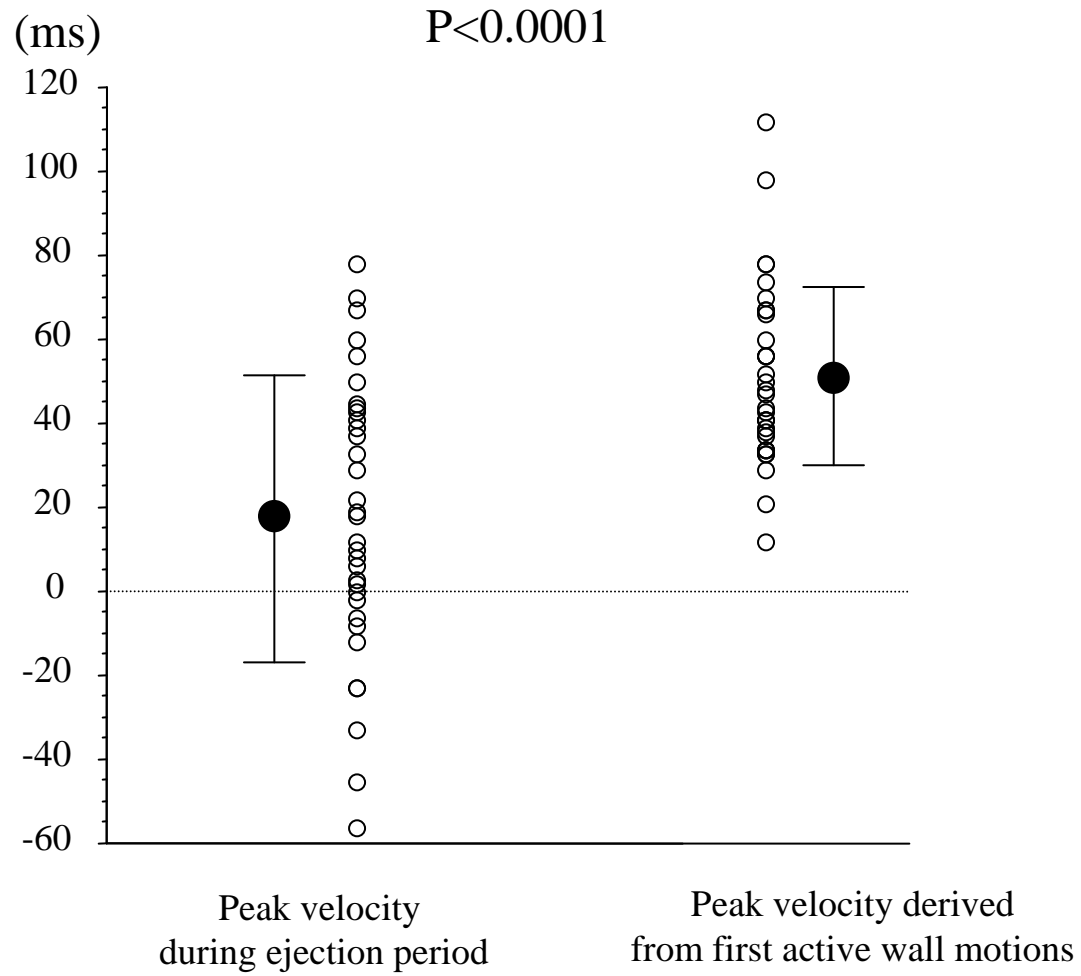


Figure 4

